

Comparisons of aerosol optical depth and surface shortwave irradiance and their effect on the aerosol surface radiative forcing estimation

Sang-Woo Kim,¹ Anne Jefferson,^{2,3} Soon-Chang Yoon,¹ Ellsworth G. Dutton,² John A. Ogren,² Francisco P. J. Valero,⁴ Jiyoung Kim,^{1,5} and Brent N. Holben⁶

Received 6 May 2004; revised 6 December 2004; accepted 12 January 2005; published 6 April 2005.

[1] Column aerosol optical depth (AOD) and surface shortwave irradiance (SSI) measurements relevant to computation of the aerosol surface radiative forcing (ΔF) and forcing efficiency (β) were taken as part of Aerosol Characterization Experiment-Asia (ACE-Asia) at the Gosan surface site in Korea in April 2001. We compare the AOD and SSI derived from three different types of Sun photometers and three sets of radiometers. We also estimate the ΔF and β using two methods and quantify the observational uncertainties of these parameters. A comparison of the AOD at 500 nm shows that the three Sun photometers generally agreed within 0.014 (mean), 0.0142 (bias), and 0.0298 (root mean square) for coincident observations. Over the course of the comparison, the mean differences between the SSI measurements were 1.6, 11.7, and 10.1 Wm^{-2} for direct, diffuse and global irradiances, respectively. However, for both the AOD and the SSI comparisons, relatively high instantaneous differences between the instruments were apparent on days with heavy dust at the surface. The mean β and associated deviations, which were estimated by the combinations of different instrument-derived AODs and SSIs, for simultaneous observation data at a 60° solar zenith angle are -79.50 ± 3.92 and $-82.57 \pm 5.70 \text{ Wm}^{-2}/\tau_{500}$ for $\text{global}_{\text{shaded}}$ (sum of direct and diffuse irradiances) and $\text{global}_{\text{unshaded}}$ (measured by the unshaded pyranometer) irradiances, respectively. The uncertainties in β associated with uncertainties in the AOD and SSI (in parentheses) for $\text{global}_{\text{shaded}}$ and $\text{global}_{\text{unshaded}}$ irradiance are about 8.6% and 3.2% (10.7%), respectively. A 2% difference between the measured global irradiances for a given 9 days was translated into an uncertainty of 19% in ΔF . This difference in ΔF between instruments caused a 14% deviation in β .

Citation: Kim, S.-W., A. Jefferson, S.-C. Yoon, E. G. Dutton, J. A. Ogren, F. P. J. Valero, J. Kim, and B. N. Holben (2005), Comparisons of aerosol optical depth and surface shortwave irradiance and their effect on the aerosol surface radiative forcing estimation, *J. Geophys. Res.*, 110, D07204, doi:10.1029/2004JD004989.

1. Introduction

[2] There is much interest in quantifying and reducing the uncertainties in calculations of the aerosol direct radiative forcing (ADRF), which is defined as the change in the global radiation balance attributable to changes in the amount of light scattered and absorbed by particles sus-

pending in the atmosphere. Despite a good understanding of how atmospheric aerosols affect the Earth's radiation budget, the ADRF has larger uncertainties than those of greenhouse gases due to the relative short lifetime, nonuniform composition, size, spatial and temporal distributions of aerosols in the troposphere [Charlson *et al.*, 1992; Schwartz and Andrea, 1996]. Add to this that aerosol properties can be difficult to measure without instrumental offsets or bias and modeling the ADRF becomes difficult.

[3] Recently, more integrated studies of aerosols were performed to reduce the uncertainties of current estimates of the ADRF such as ACE-1 [Bates *et al.*, 1998], ACE-2 [Raes *et al.*, 2000], ACE-Asia [Huebert *et al.*, 2003], INDOEX [Ramanathan *et al.*, 2001] and TARFOX [Russell *et al.*, 1999]. In spite of numerous studies, there are substantial differences in ADRF estimates due to intrinsic errors in the observations and modeling. According to results from the Asian Pacific Regional Aerosol Characterization Experiment (ACE-Asia), which took place during the spring of 2001, the aerosol-induced radiative flux changes at the

¹School of Earth and Environmental Sciences, Seoul National University, Seoul, Republic of Korea.

²NOAA Climate Monitoring and Diagnostics Laboratory, Boulder, Colorado, USA.

³Also at Cooperative Institutes for Research in Environmental Sciences, University of Colorado, Boulder, Colorado, USA.

⁴Scripps Institution of Oceanography, University of California, San Diego, La Jolla, California, USA.

⁵Also at Meteorological Research Institute, Korea Meteorological Administration, Seoul, Republic of Korea.

⁶NASA Goddard Space Flight Center, Greenbelt, Maryland, USA.

surface, in terms of aerosol surface radiative forcing (ΔF , defined as the difference between the net radiative flux calculated with and without aerosols) and forcing efficiency (β , defined as ΔF per unit aerosol optical depth), varied by tens of watts per square meter for the ACE-Asia region and were strongly perturbed by the varying aerosol loadings and types, surface albedo and relative humidity [Huebert *et al.*, 2003; Markowicz *et al.*, 2003]. Calculations of the daily mean ΔF with heavy dust loading differ by -58.1 W/m^2 and -52.1 W/m^2 on a day with heavy dust loading (DOY (day of year) 103, 2001), and, inversely, -29.0 W/m^2 and -34.0 W/m^2 on relatively clean day (DOY 105, 2001) by Won *et al.* [2004] and Bush and Valero [2003], respectively. In addition to the variability in the aerosol loadings, the estimated ΔF shows distinct differences due to different observational instruments, analytical periods and methods. For example, clear-sky shortwave ΔF at Gosan had a value of -30.5 W/m^2 from ground-based measurements from 25 March to 4 May 2001 [Bush and Valero, 2003], while an NCAR CRM simulation for April 2001 (16 days) estimated the value as -46.5 W/m^2 [Won *et al.*, 2004]. Nakajima *et al.* [2003] estimated a ΔF of $-25.9 \pm 8.3 \text{ W/m}^2$ from surface measurements, $-30.7 \pm 11.8 \text{ W/m}^2$ by satellite measurement, $-19.8 \pm 11.0 \text{ W/m}^2$ from the CFORS mesoscale chemical model and $-21.6 \pm 7.8 \text{ W/m}^2$ from the SPRINTARS model simulation for April 2001. These differences in the ΔF at Gosan site described in the above measurement and model studies stress the necessity of more accurate measurements of the aerosol optical properties (e.g., aerosol optical depth, single scattering albedo) and the surface solar irradiance before employing them in radiative transfer model simulations to reduce uncertainties in the ADRF.

[4] In this study, we present comparisons of the aerosol optical depth (AOD) and the surface solar irradiance (SSI) measured from three, independently calibrated, Sun photometers and sets of radiometers at Gosan during the ACE-Asia field campaign. From these measurements, we compute values of ΔF and β with two objectives: (1) to investigate how precisely we can measure the AOD and SSI from current radiometers over a broad range of aerosol loading conditions, and (2) to quantify how observational errors affect estimates of ΔF and β .

[5] Since the mid-1990s several networks for aerosol optical properties and solar radiation measurements have operated globally; e.g., respectively AERONET [Holben *et al.*, 1998] and Baseline Surface Radiation Network (BSRN) [Ohmura *et al.*, 1998]. To evaluate the quality of data from global networks a comparison across various atmospheric conditions is needed because the spatial and temporal distributions of aerosol loadings and compositions in the troposphere are highly varied. However, to date, most intercomparison studies of the AOD and SSI have been made under clean atmospheric conditions for accurate calibration [McArthur *et al.*, 2003; Michalsky *et al.*, 1999; Mitchell and Forgan, 2003; Schmid *et al.*, 1999]. Comparisons of the AOD and SSI under a broad range of aerosol loadings are needed to verify the consistency of data from the various instruments before employing them in an assessment of the observational uncertainties in the ADRF.

[6] This paper investigates the performance of current radiometric measurements at Gosan, South Korea, where AOD levels are 0.03–1.1 in the midvisible, and their effect

on estimations of the ΔF and β . Section 2 gives brief descriptions of the instruments used in this study. In sections 3 and 4, we present comparisons of the AOD and SSI derived from independently calibrated Sun photometers and radiometers. We discuss the source of discrepancies and suggest what factors might help to reduce them. In section 5, we present calculations of the ΔF and β using two analytical methods, a direct approach using only measurements and a hybrid method which combines measurements and model calculations. We discuss the sensitivity of ΔF and β to the AOD and to the SSI. In the final section, we summarize and discuss how these results can be applied to minimize the observational errors to improve estimates of ΔF and β .

2. Measurements

2.1. Aerosol Optical Depth

[7] Aerosol optical depth (AOD) is a critical parameter in estimating the transmission of solar radiation throughout Earth's atmosphere. Sun photometers are commonly used to evaluate the spectral AOD in many ground-based monitoring programs and intensive field campaigns. During the ACE-Asia intensive observation period (IOP), measurements of the AOD were made at the Gosan surface site (33.29 N, 126.16 E, 71 m above MSL) by three different Sun photometers. The next section gives brief descriptions of each instrument used in this study and highlights the important points (e.g., data retrieval process, calibration) needed for intercomparison and the ΔF and β estimation.

2.1.1. Retrieval Processing and Calibration

[8] Optical depth, τ_λ , at a central wavelength λ , can be derived from the Beer-Bouguer-Lambert's law in the form [Dutton *et al.*, 1994]:

$$I(\lambda) = E_o I_o(\lambda) e^{-m\tau(\lambda)}, \quad (1)$$

where $I(\lambda)$ is the measured instrument voltage, E_o is a correction factor for variations in the Sun-Earth distance, m is the refracted path length through the atmosphere when the measurement is made, $\tau(\lambda)$ is optical depth at a central wavelength λ and $I_o(\lambda)$ is the extraterrestrial flux in unit of volts. Of critical importance to any Sun photometer measurement is the calibration of each instrument under stable, clean and cloud-free atmospheric conditions. The mean voltage of extrapolated zero air mass in the Langley plot (air mass versus $\ln I(\lambda)$), selected for near ideal days, is the calibration constant used when evaluating solar attenuation at any specific wavelength. In converting the radiation measurement data, the raw signal obtained from ground-based Sun photometer to optical depth, the data retrieval and calibration process all contribute to the accuracy of the AOD. From equation (1), spectral total optical depth, represented as the sum of atmospheric constituents, is as follows:

$$\tau(\lambda) m = \sum \tau_i(\lambda) m_i. \quad (2)$$

[9] To obtain the AOD from equation (2), it is necessary to consider the wavelength-dependent attenuation of solar radiation by minor constituents of the atmosphere, subscript i symbol. In this study, no agreed upon protocol was

Table 1. Instrumentations of Aerosol Optical Depth Measurement

Sun Photometer	Institute	Wavelength, λ nm	FWHM, nm	FOV	Accuracy
Carter-Scott SP 02 (No. 1026)	CMDL	412, 500, 675, 862	10	2.5°	± 0.02
Carter-Scott SP 022 (No. 1027)	CMDL	368, 500, 610, 778	10	2.5°	± 0.02
Eko MS-110	METRI	368, 500, 675, 778, 862	5	2.5°	± 0.02
Cimel 318-1	AERONET	340, 380, 440, 500, 670, 870, 1020	10	1.2°	± 0.01

developed for removal of gas phase constituents and Rayleigh scattering as well as cloud screening of data. Each data set was corrected for these factors independently. Consequently, there will be differences based on the precision of the Rayleigh and ozone optical depth calculation.

2.1.2. Instrumentation and Accuracy

[10] In recent years, great progress has been made to capture current and recent-past aerosol variability through globally diverse AOD networks such as AERONET [Holben *et al.*, 1998], SKYNET [Kim *et al.*, 2004] and AEROCAN [Bokoye *et al.*, 2001]. A summary of the instruments used in this study is given in Table 1. A description of each instrument, measurement sequences, accuracy and cloud-screen procedure follows.

[11] The National Oceanic and Atmospheric Administration (NOAA) Climate Monitoring and Diagnostics Laboratory (CMDL) deployed two Carter-Scott four-channel Sun photometers, SP02 and SP022, mounted on a Sci-Tech active solar-seeking tracker at the top of a 30 m tower during the ACE-Asia IOP. The solar-tracker moves under computer control and an active solar position feedback sensor, which keeps the CMDL Sun photometers aligned to the Sun, centered to within 0.1° of the true center of the field-of-view (FOV) in clear sky. The CMDL Sun photometer collected data at 368, 412, 500, 610, 675, 778 and 862 nm wavelengths for a duration of one second once per minute. The 500 nm channel is an identical wavelength of the two CMDL Carter-Scott Sun photometers. The 500 nm AOD value used in this study was calculated from a fit of the 7 wavelength channels. Because AOD is a smoothly varying function of wavelength, a fit to all the channels, one of which is 500 nm, can be a better estimate of the 500 nm values than just the single measurement and can avoid unusual peaks in the AOD spectrum. The reported accuracy of the spectral AOD is approximately 0.02. Calibration of the CMDL Sun photometers was performed at the NOAA/CMDL facilities (39.99 N, 105.26 W, 1700 m above MSL) using a Langley plot approach before and after the ACE-Asia IOP. On-site personnel provided cleaning and maintenance of the field instruments.

[12] The Aerosol Robotic Network (AERONET) is a globally distributed, ground-based network of seven-channel cimel 318-1 Sun/sky radiometers [Holben *et al.*, 1998]. AERONET Sun photometer measurements were taken at the top of a container (3.5 m above ground level, at a distance of 15 m from the tower) from 4 April to 20 June 2001. The AERONET Sun photometer collected AOD once every 15 min. These data were cloud screened and processed through an inversion algorithm [Smirnov *et al.*, 2000; Dubovik and King, 2000]. The measurements have a reported accuracy of ± 0.01 AOD [Dubovik *et al.*, 2000]. In this study, level 2.0 data at 340, 380, 440, 500, 670, 870 and 1020 nm wavelengths were downloaded from <http://aeronet.gsfc.nasa.gov>.

[13] The Meteorological Research Institute (METRI) five-channel Sun photometer (EKO, MS110) was situated at the top of the Gosan weather station building (90 m above MSL), which is located about 100 m northeast of the CMDL and AERONET Sun photometers. The METRI Sun photometer made spectral AOD measurements at 368, 500, 675, 778 and 862 nm wavelengths for a time period of 1 s once per minute from 1 March to 4 May 2001. Details of the cloud screen and data retrieval processes can be found in the work of Min *et al.* [2002].

[14] In this study, the 500 nm AOD used for the comparison amongst Sun photometers and estimates of ΔF and β were filtered: if the differences in the AOD between instruments were greater than 0.5 and exceeded three standard deviations from the overall mean AOD difference, the observation pair was eliminated.

2.2. Surface Shortwave Irradiance

[15] The measurements of downwelling solar fluxes presented in this paper were made at the same locations as the AOD measurements by three different groups of instruments operated by CMDL, Scripps Institute of Oceanography (SIO) and METRI, respectively.

[16] All of the SSI measurements by CMDL are made in accordance with specifications of the World Climate Research Program's Baseline Surface Radiation Network (BSRN) [Ohmura *et al.*, 1998]. CMDL SSI data are composed of the sum of two components of solar irradiance, direct and diffuse, in broad wavelength bands (0.2–4.0 μm) [Michalsky *et al.*, 1999]. Direct normal irradiance was measured by a pair of pyrhemometers, an Eppley normal incidence pyrhemometer (field-of-view (FOV): $\pm 2.8^\circ$) and a Kipp and Zonen CH-1 pyrhemometer (FOV: $\pm 2.5^\circ$). Diffuse irradiance was measured by a pair of shaded pyranometers, an Eppley 8–48 black and white and a Kipp and Zonen CM22, whose dome and receiver was shaded from the direct solar beam by a tracking disk. For both direct and diffuse irradiance measurements the higher values of the two instruments was used in this study. From the direct measurements 69.8% of the data came from the Eppley normal incident pyrhemometer and 30.2% from the Kipp and Zonen CH-1 pyrhemometer. In case of diffuse irradiance, the 99.9% of data came from the Eppley PSP 8–48 black and white pyranometer. The downwelling global solar irradiance is the sum of the direct normal irradiance multiplied by the cosine of solar zenith angle (SZA) and the diffuse irradiance. The instrument calibrations are traceable to the World Radiation Reference (WRR) standard. The accuracy is about 10 W/m^2 for the 1-min averages recorded from 1 Hz sampling rate. Significant flux uncertainties of the pyranometer measurements may result from temperature and angular (or azimuthal) responses of the instrument. The cosine response problem is avoided by using the sum of the diffuse and direct where cosine errors become very small or

Table 2. Instrumentations of Surface Solar Irradiance Measurement

Radiometer	Institute	Band Pass, μm	FOV
<i>Direct Component</i>			
Eppley normal incidence pyrheliometer	CMDL	0.285–4.0	$\pm 2.8^\circ$
Kipp and Zonen CH-1 normal incidence pyrheliometer	CMDL	0.2–4.0	$\pm 2.7^\circ$
Direct total solar broad and radiometer (DTSBR)	SIO	0.3–3.8	$\pm 2.8^\circ$
<i>Diffuse Component</i>			
Eppley 8–48 black and white pyranometer	CMDL	0.285–2.8	hemispheric cosine response shade disk
Kipp and Zonen CM22 pyranometer	CMDL	0.2–3.6	hemispheric cosine response shade disk
<i>Global Component</i>			
EKO MS-801 pyranometer	METRI	0.3–2.8	hemispheric cosine response
Total solar broadband radiometer (TSBR)	SIO	0.3–3.8	hemispheric cosine response

negligible [Michalsky *et al.*, 1999]. The pyranometers were also corrected of thermal offset errors [Dutton *et al.*, 2001].

[17] SIO deployed the TSBR (Total Solar Broadband Radiometer) and Direct TSBR (DTSBR). TSBR covered a wavelength region from approximately 0.3 to 3.8 μm with a hemispherical FOV. DTSBR, mounted on a solar tracker, was the same radiometer as TSBR except for its FOV: $\pm 2.8^\circ$. These two instruments give a direct measurement of the direct and global components of the solar flux. The absolute accuracy of the two broadband radiometers has a 1% uncertainty [Bush and Valero, 2002]. Here, unlike the CMDL measurement approach, the diffuse component is determined by subtracting the direct component from the global component.

[18] METRI made global component measurement of the total solar irradiance at the same location as the METRI Sun photometer with a single EKO MS-801 pyranometer from 1 March to 4 May 2001. The METRI pyranometer band pass covered from approximately 0.3 to 2.8 μm with a hemispherical FOV.

[19] A summary of radiometers used in this study is given in Table 2. To distinguish between the total solar irradiance between CMDL and SIO/METRI radiometers, we represent the CMDL global component, sum of direct and diffuse irradiance, as $\text{global}_{\text{shaded}}$ irradiance and the SIO/METRI global component as $\text{global}_{\text{unshaded}}$ irradiance in this study. These three sets of radiometers allow an independent evaluation of the uncertainty in the SSI measurements. Like the AOD comparison, the observation data pair was removed before comparison statistics if the difference between SSI exceeded 100 W/m^2 or three standard deviations from the overall mean SSI.

3. Aerosol Optical Depth Comparison

[20] Recent intercomparisons of AODs as derived from simultaneous observations of Sun photometers were performed for periods of several days to several months under relatively clean atmospheric conditions [e.g., Schmid *et al.*, 1999; McArthur *et al.*, 2003; Mitchell and Forgan, 2003]. This study documents a comparison of AOD between three Sun photometers from 5 April to 4 May at Gosan, where 500 nm AOD levels varied from 0.05 to 1.0 over the course of the ACE-Asia campaign. Comparisons were made for 500 nm, which is an identical wavelength of each instrument (see Table 1) and for both the total observation data (hereafter called, TOD) and also for near simultaneous

observation data (hereafter called, SOD) which is for data collected less than 10 s apart.

[21] Figure 1 shows the statistical comparison of AOD at 500 nm wavelength (τ_{500}) measured by the CMDL, METRI, and AERONET Sun photometers from 5 April to 4 May 2001. For the TOD in Figure 1a, both the mean τ_{500} values and the spread between the 25th and 75th percentiles of the AERONET data are higher than those of CMDL and METRI. However, both the mean τ_{500} values and the range of percentiles are nearly identical for SOD. The maximum variance of the mean τ_{500} between instruments is 0.038 and 0.014 for TOD and SOD, respectively. The number of data points in TOD varied by as few as 544 for AERONET to as high as 6109 for METRI. This discrepancy results from the number of days of operation, incomplete cloud screening as well as the instrument operating in either periodic or continuous measurement modes.

[22] Table 3 lists the bias difference (BD), root mean square difference (RMSD), standard deviation of difference (SDD), slope and intercept for the best fit line, and number of observations (N) for the various combinations of instruments shown in Figure 1b. The results of AOD over a broad range of aerosol loadings at Gosan indicate that the τ_{500} obtained from the three instruments compare well. The CMDL and METRI Sun photometers show an agreement of 0.006 (BD) and 0.030 (RMSD). A positive BD indicates that the τ_{500} of Sun photometer A is lower than the Sun photometer B. The AOD derived from the AERONET instrument are greater than those of CMDL and METRI. The BD, RMSD and SDD of present comparisons lie in the range -0.014 – 0.078 , 0.023 – 0.030 and 0.018 – 0.030 , respectively. These values are similar to or slightly larger than previous comparison studies [i.e., Schmid *et al.*, 1999; McArthur *et al.*, 2003; Mitchell and Forgan, 2003].

[23] Although the statistical comparisons are within the reported instrumental uncertainties, noticeable differences in the instantaneous data points of τ_{500} are apparent. Figure 2a shows the scatterplot of τ_{500} of SOD for the METRI (circle) and AERONET (cross hair) Sun photometers relative to the CMDL Sun photometer. The majority of the τ_{500} ranged from 0.25 to 0.5. In this majority range, the CMDL τ_{500} is slightly lower than that of AERONET, but slightly higher than the METRI τ_{500} . The CMDL τ_{500} shows lower values at high aerosol loadings (e.g., $\tau_{500} > 0.7$), but higher values below an AOD of 0.3. These differences of τ_{500} over a broad range of aerosol loadings are more clearly shown in Figure 2b. Figure 2b shows the absolute differences be-

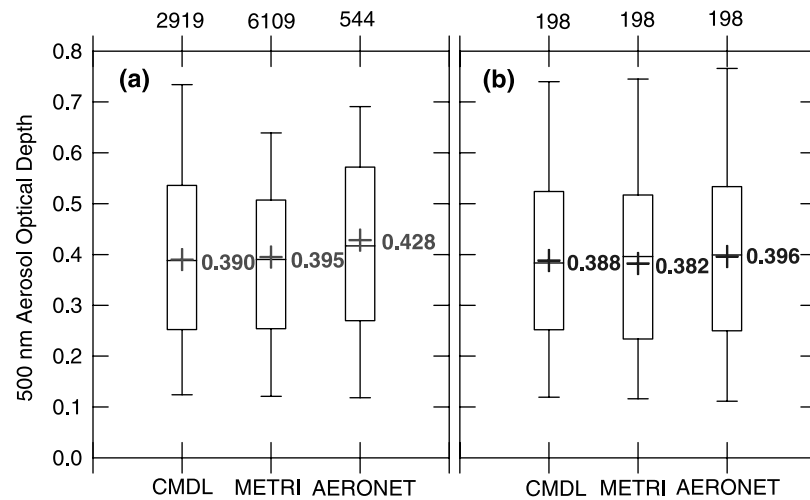


Figure 1. Statistical comparison of the CMDL, METRI, and AERONET Sun photometer-derived 500 nm aerosol optical depths: (a) total and (b) simultaneous observation data from 5 April to 4 May 2001. The top and bottom of error bars are the 95th and 5th percentiles; the top and bottom of box are the 75th and 25th percentiles; a line and cross in the box represent the median and mean values, respectively. The mean values of 500 nm AOD and sample size in each distribution are shown on the right of box and at the top, respectively.

tween CMDL and METRI and AERONET τ_{500} . On 13 April (DOY 103), the micropulse lidar (MPL) observed an immense Asian dust layer both aloft and at the surface [Yoon *et al.*, 2001]. On this day, the AERONET and METRI AOD values are as much as 0.09 higher than that of CMDL.

[24] The lower response of the CMDL τ_{500} during this high dust-loading day could be due in part to the instrument location on top of a 30 m tower. On day 103 relatively high surface aerosol extinction coefficients with an average value of 0.440 km^{-1} at 550 nm were reported from in situ observations of ambient sub $10 \mu\text{m}$ size particles. The actual aerosol extinction near the surface may have been as high as 0.8 km^{-1} for shorter periods. However, even with an extinction coefficient at 500 nm as high as 1.0 km^{-1} this would only account for a difference of 0.03 AOD between the CMDL instrument at the top of the tower and those closer to the surface. Another condition that may have affected the AOD measurements on this day is the time of the daily instrument cleaning. This day was particularly dusty with high wind speeds ($8 \sim 13 \text{ m/s}$). Radiometer surfaces may have been coated with a substantial dust layer over a period of a few hours, giving anomalously high AOD values. Because no large decline in the AOD was observed after a radiometer cleaning we cannot ascertain the magnitude of this error. Day 103 had high winds, with gusts up to 25 ms^{-1} . The radiometers near the surface may have been more susceptible to surface dust accumulating on the radiometer surface than the CMDL radiometer on top of the

30m tower. These differences of τ_{500} between instruments exceed the reported observational accuracies of each instrument and may arise from differences in the field maintenance and measurement elevation on this day. Therefore, to avoid anomalously high or low AOD values we recommend that instruments be colocated near to the surface and undergo frequent cleaning.

[25] In addition, an interesting feature of the comparison is small difference in the low AOD (Figures 1 and 2a). Compared to the previous studies [i.e., McArthur *et al.*, 2003; Mitchell and Forgan, 2003] under extremely low aerosol loads, an AOD comparison like this study, which takes place under varying aerosol loadings, is preferable to verify the consistency of measurements.

[26] Because the AOD is a critical parameter in radiative transfer calculations of the SSI and in estimation of β , the observational differences in the instantaneous AOD between the instruments at a low or high aerosol loading conditions translates into large differences in ΔF and β . The propagation of the variance between instrument AOD values in the ΔF and β uncertainties is assessed in section 5.

4. Surface Shortwave Irradiance Comparison

[27] Because there are both discrepancies [Kato *et al.*, 1997; Halthore *et al.*, 1998] and good agreements [Chou and Zhao, 1997; De La Casinière *et al.*, 1997] between modeled and measured solar fluxes, determination of the

Table 3. Bias Difference, Root Mean Square Difference, Standard Deviation of the Difference, Slope and Intercept of the Best Fit Line, and Number of Observations Between Sun Photometer A and B in the 500 nm AOD Comparison^a

Sun Photometer A	Sun Photometer B	BD	RMSD	SDD	Slope	Intercept	N
CMDL	METRI	-0.0064	0.0298	0.0298	1.0199	-0.0141	198
CMDL	AERONET	0.0078	0.0231	0.0218	1.0633	-0.0168	198
AERONET	METRI	-0.0142	0.0230	0.0182	0.9627	0.0006	198

^aAbbreviations are as follows: BD, bias difference; RMSD, root mean square difference; SDD, standard deviation of the difference; and N, number of observations. The Sun photometer A was chosen as the reference instrument. BD and RMSD are $\frac{1}{N} \sum (B_i - A_i)$ and $\sqrt{\frac{1}{N} \sum (B_i - A_i)^2}$, respectively. The slope and intercept are calculated as $B = \text{slope} \times A + \text{intercept}$.

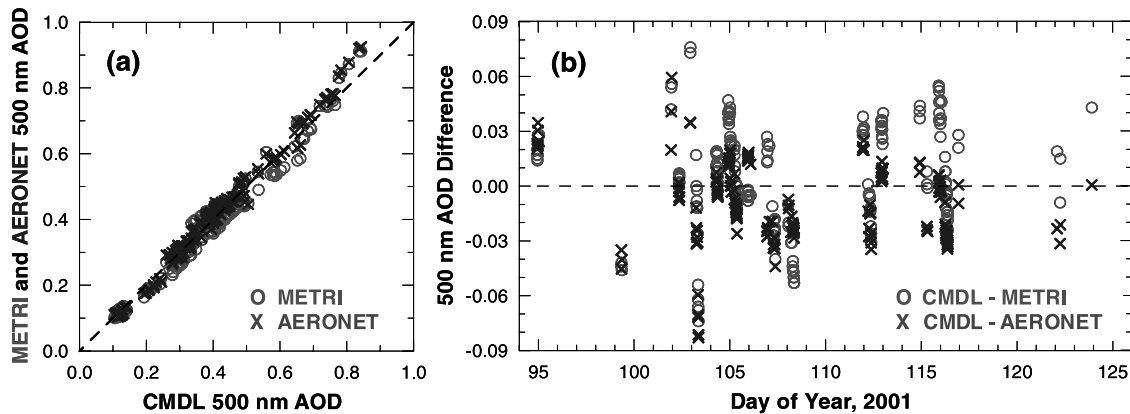


Figure 2. (a) Scatterplot of τ_{500} for the METRI (circle) and AERONET (cross hair) Sun photometers relative to the CMDL Sun photometer and (b) the absolute differences between CMDL, METRI, and AERONET τ_{500} of SOD from 5 April to 4 May 2001.

surface shortwave irradiance (SSI) using a radiation model remain uncertain either due to inaccurate measurements, poor model parameterizations or both. These previous results motivated us to study the observational uncertainties of SSI measurements of different radiometers before looking at the model-calculated downwelling SSI.

[28] Tables 4a and 4b show the statistical comparisons of the direct, diffuse and global solar irradiance for SOD at Gosan during the ACE-Asia IOP. In the direct solar irradiance measurements, the CMDL and SIO radiometers had excellent agreement of their mean values with 1.6 W/m^2 difference, and also had a small bias, BD of 1.582. This result is comparable to that listed by Michalsky *et al.* [1999], who obtained agreement within $\pm 3 \text{ W/m}^2$ for five instruments. Candidates for the possible differences between the direct beam instruments are tracking errors and cleaning of the radiometer surface.

[29] The absolute difference between the mean CMDL $\text{global}_{\text{shaded}}$, SIO $\text{global}_{\text{unshaded}}$ and METRI $\text{global}_{\text{unshaded}}$ irradiance is about 10 W/m^2 with a BD of approximately 10.0 and a RMSD of 13.0. The mean and BD between the SIO and the METRI $\text{global}_{\text{unshaded}}$ irradiances show good agreement, despite relatively large values of RMSD and SDD. These differences agree within reported instrument uncertainties and are consistent with a comparable study [Michalsky *et al.*, 1999].

[30] The difference between the CMDL $\text{global}_{\text{shaded}}$ and SIO $\text{global}_{\text{unshaded}}$ component of the solar irradiance depends on the diffuse radiation comparison in this study. The diffuse averages are 199.3 and 187.6 W/m^2 for CMDL and SIO with -11.629 (BD) and 14.146 (RMSD). Because the SIO diffuse irradiance is calculated as the difference of global and direct irradiances, a small percentage error in the global irradiance can become a large percentage error in the diffuse irradiance.

[31] The CMDL $\text{global}_{\text{shaded}}$ irradiance, which is the sum of direct and diffuse irradiance, was higher than SIO and METRI, which deployed a single hemispheric FOV radiometer to measure the $\text{global}_{\text{unshaded}}$ irradiances. The error in CMDL $\text{global}_{\text{shaded}}$ measurement is a combination of the error in the direct beam as described above and that in the measured diffuse. Errors in the diffuse irradiance measured by a shaded pyranometer and in the global irradiances

measured by the stand-alone hemispheric FOV radiometers result from an offset due to thermal IR exchange between the detector and filter domes [Dutton *et al.*, 2001; Philipona, 2002], tracking errors and an instrument cosine response error, which is caused by the anisotropic diffuse solar field [Michalsky *et al.*, 1999, 2003]. Like the AOD comparison, a significant difference between direct shortwave irradiance was found during the Asian dust day, on 13 April (DOY 103). Figure 3 shows the absolute differences of the direct, diffuse and global irradiances between radiometers plotted as a function of day of year under clear sky conditions. As noted above, a wide variety of sky conditions existed during the comparison periods. In Figure 3a, differences between the CMDL and SIO direct shortwave irradiances varied by no more than 2.5% except for day 103 when an Asian dust storm passed through the region. The maximum difference between the CMDL and SIO direct solar irradiances was near 8% with CMDL having a lower value on 13 April. In contrast, the CMDL diffuse and $\text{global}_{\text{shaded}}$

Table 4a. Statistical Comparisons of Surface Solar Irradiance (W/m^2) for Simultaneous Observation Data at Gosan From 5 April to 4 May 2001

	Direct		Diffuse		$\text{Global}_{\text{shaded}}^{\text{a}}$		$\text{Global}_{\text{unshaded}}^{\text{a}}$
	CMDL	SIO	CMDL	SIO	CMDL ^b	SIO ^c	METRI
Mean	304.6	305.8	196.3	185.7	500.9	491.5	490.6
Median	284.2	285.8	200.2	189.7	480.8	474.4	472.5
Std	177.6	177.4	66.3	63.4	209.6	206.1	210.3
Max.	903.8	902.6	362.7	354.4	1016.5	995.2	1013.1
Min.	15.3	16.4	56.7	53.7	86.2	83.3	77.0
N	1461	1461	1461	1461	1461	1461	1461

^aTo distinguish the measurement of downwelling total solar irradiance of CMDL and SIO/METRI radiometers, we represent CMDL $\text{global}_{\text{shaded}}$ irradiance as $\text{global}_{\text{shaded}}$ irradiance and SIO (measured by a TSBR) and METRI (measured by the unshaded pyranometer) $\text{global}_{\text{unshaded}}$ irradiance as $\text{global}_{\text{unshaded}}$ irradiance.

^bThe CMDL $\text{global}_{\text{shaded}}$ irradiance is the sum of the vertical component of the direct irradiance measured by a tracking pyrheliometer and the diffuse horizontal irradiance measured by a pyranometer whose dome and receiver are shaded by a tracking disk [Ohmura *et al.*, 1998].

^cUnlike the CMDL measurement, SIO measured the direct and global components. The diffuse irradiance was determined by subtracting the direct irradiance from the global irradiance.

Table 4b. Statistical Comparisons of the Surface Solar Irradiance (W/m^2) for Simultaneous Observation Data at Gosan From 5 April to 4 May 2001

	Direct CMDL ^a SIO	Diffuse CMDL SIO	Global		
			CMDL SIO	CMDL METRI	SIO METRI
BD	1.2405	-10.6381	-9.3913	-10.3096	-0.9182
RMSD	2.7342	12.4732	11.8351	13.1094	7.1718
SDD	2.4374	6.5248	7.2048	8.1003	7.1153
Slope	0.9992	0.9512	0.9828	1.0026	1.0200
Intercept	1.4896	-1.0546	-0.7790	-11.5910	-10.7460

^aThe left instrument was chosen as the reference instrument.

irradiance were slightly higher than that of SIO and METRI, in the afternoon on day 103. One possibility for the discrepancy on day 103 is the time of day that the radiometers were checked and cleaned. Another candidate for the difference on 13 April is the solar-tracking accuracy in the direct and diffuse irradiance measurements. The solar-tracking accuracy requirement is based on the relationship between the effective FOV of most pyrheliometers (about 1°) and the actual diameter of the Sun's disk (about 0.5°). Hence in high AOD situations, e. g., on 13 April when the mean τ_{500} was 0.738 ± 0.036 , minor changes in pointing accuracy can affect the uncertainties in the direct solar

signal centered on the Sun [Ohmura *et al.*, 1998]. Tracking errors in the diffuse measurements can also occur, especially if the shading balls of the tracker are not centered on the radiometers. High wind speed (10.7 ± 1.5 m/s) on this day added more difficulty to the instrument tracking.

[32] In the diffuse and global irradiance difference between CMDL and SIO, a distinct diurnal variation is apparent on days 105, 106, 107, 108, 112, and 116, with CMDL having higher values. The strong solar zenith angle (SZA) dependence of differences between CMDL and SIO in Figures 3b and 3c, maximum near local solar noon (low SZA), may come from the cosine response errors of both the

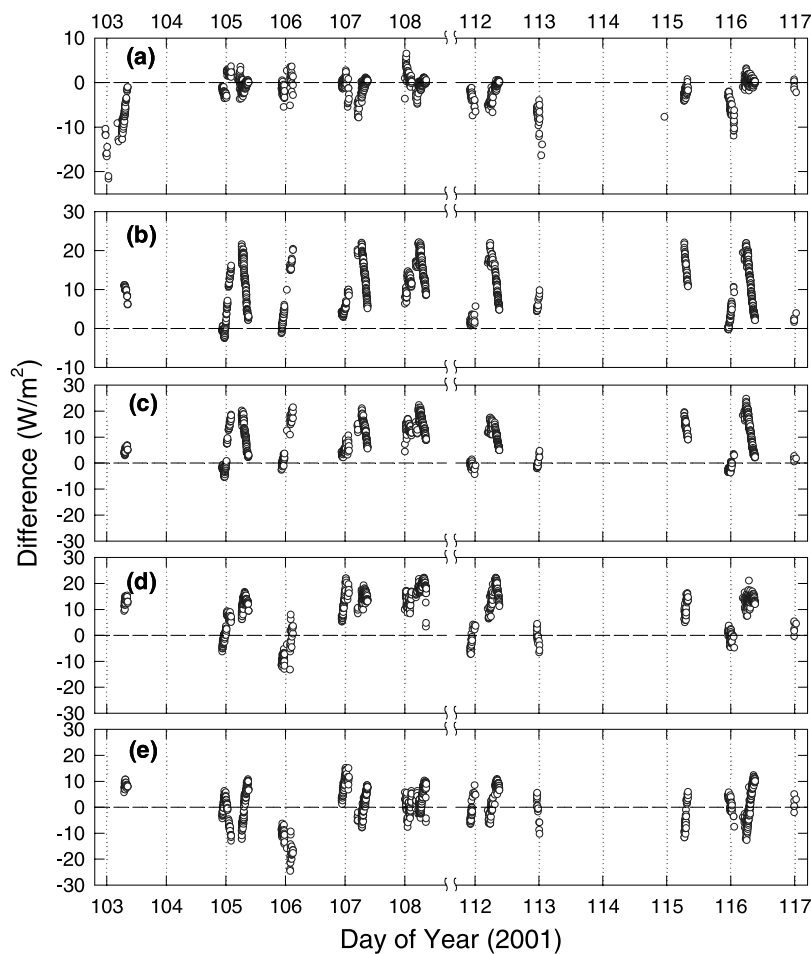


Figure 3. Absolute difference of surface shortwave irradiances between instruments plotted as a function of day of year: (a) direct, CMDL minus SIO; (b) diffuse, CMDL minus SIO; (c) global, CMDL minus SIO; (d) global, CMDL minus METRI; and (e) global, SIO minus METRI.

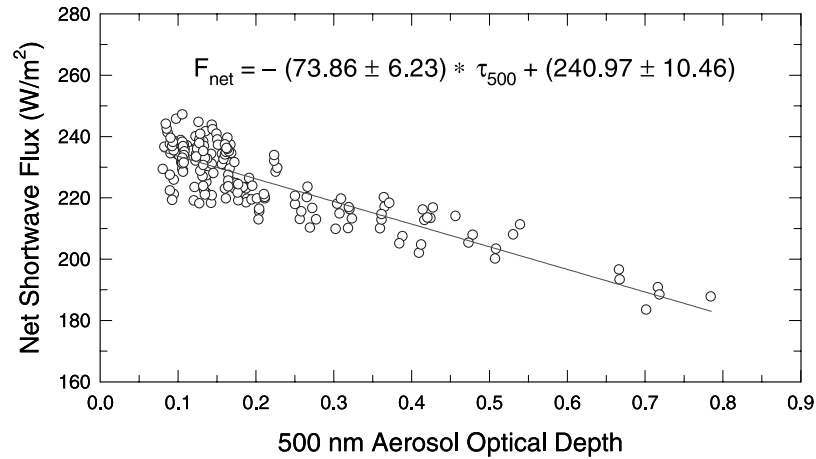


Figure 4. Scatterplot of the CMDL net solar flux versus 500 nm AOD at 60° solar zenith angle at Gosan from April 2002 to January 2003.

CMDL and SIO instruments. The effects of thermal offset errors of both instruments and inadvertent shadowing of the CMDL diffuse radiometers are expected to be small. Meanwhile, the difference between CMDL and METRI in Figure 3d showed a small bias in the morning and a large bias in the afternoon, but no distinct diurnal variation. The percent difference (not shown) gradually increased with time in the afternoon or with SZA. The reason for this tendency is unclear in this study.

[33] The differences of SSI between instruments described in this section will considerably affect the ΔF and β when we combine each instrument-measured SSI and AOD. The propagation of the variance is assessed in section 5.

5. Sensitivity of Aerosol Radiative Forcing to Aerosol Optical Depth and to Surface Shortwave Irradiance Measurements

[34] Both ΔF and β presented in this section were estimated from AOD and SSI measurements as described in sections 3 and 4. The following is an evaluation of the effect of how errors in the measurements of AOD and SSI affect derivations in ΔF and β using the direct and hybrid analytical methods.

5.1. Direct Method: Net Solar Flux Versus AOD Approach

[35] The direct method uses a regression of the net solar flux versus the AOD to estimate the instantaneous β . The broadband net solar flux, F_{net} (W/m^2), is calculated as [Bush and Valero, 2002]:

$$F_{\text{net}} = (1 - \alpha) \times F, \quad (3)$$

where F is the measured SSI and α is surface albedo. The advantage of this method is that it avoids dependence on a radiative transfer model calculation.

[36] Figure 4 is a scatterplot of the net solar flux as a function of τ_{500} at a 60° SZA measured by the CMDL instruments at Gosan from April 2001 to January 2002. The slope of the linear fit of cloud-screened data is β . Here, β for the $\text{global}_{\text{shaded}}$ irradiance is $-73.86 (\pm 6.23) \text{ Wm}^{-2}/\tau_{500}$.

[37] To evaluate the effects of the observational uncertainties amongst different instruments on β , β s were calculated using combinations of the three Sun photometer-derived AODs and respective SSI values. Figure 5 shows estimates of β at a 60° SZA for both TOD and SOD. Overall, there is fair agreement in estimates of β for both data sets despite use of various combinations of AOD and SSI. The mean β s of SOD are -411.14 , 126.46 , -79.50 and $-82.57 \text{ Wm}^{-2}/\tau_{500}$ for direct, diffuse, $\text{global}_{\text{shaded}}$ and $\text{global}_{\text{unshaded}}$ irradiances, respectively. The percent deviations of β relative to the mean values for SOD are 2.6%, 4.5%, 4.8% and 6.9% for direct, diffuse, $\text{global}_{\text{shaded}}$ and $\text{global}_{\text{unshaded}}$ irradiances, respectively. The average squared deviation of β relative to the mean values or variance due to different AOD measurements for direct, diffuse, $\text{global}_{\text{shaded}}$ and $\text{global}_{\text{unshaded}}$ irradiances are 4.3%, 4.8%, 8.6% and 3.2%, respectively. Whereas, the variance of β from the mean value due to different SSI measurements is 1.9%, 2.7% and 10.7% for the direct, diffuse and $\text{global}_{\text{unshaded}}$ irradiances, respectively. The difference between the $\text{global}_{\text{shaded}}$ and $\text{global}_{\text{unshaded}}$ irradiance on β is about 6.9% relative to the mean β of $\text{global}_{\text{shaded}}$ irradiance.

5.2. Hybrid Method: Aerosol Radiative Forcing (ΔF) Versus AOD Approach

[38] The hybrid method uses the instantaneous ΔF and AOD. The instantaneous ΔF for a given observation site and time is estimated as follows [Bush and Valero, 2002]:

$$\Delta F = (1 - \alpha) \times (F - F^\circ) \quad (4)$$

where F° is the SSI in pristine (aerosol-free) atmospheric conditions. In this study, the direct, diffuse and global components of the SSI under aerosol-free conditions, F° , were evaluated with the radiative transfer model SBDART (Santa Barbara DISORT atmospheric radiative transfer, version 2.0) which is based on the DISORT algorithm for discrete ordinate method radiative transfer in multiple scattering and emitting layered media [Ricchiuzzi et al., 1998]. The advantage of the hybrid method is that measurements of complicated aerosol properties are not necessary. In the hybrid method, the model-calculated SSI is most sensitive to the surface albedo, atmospheric gases and

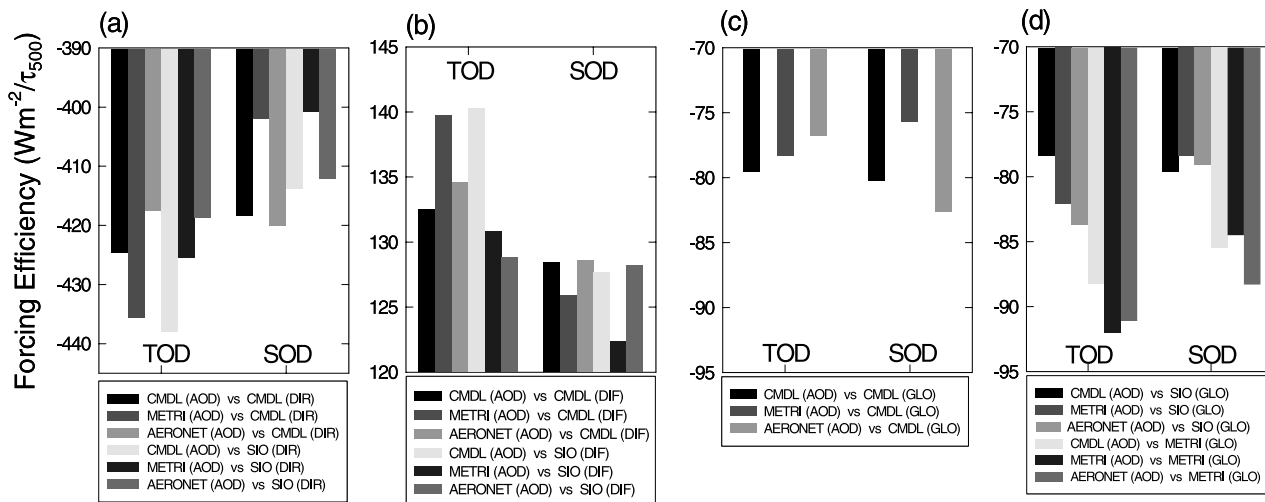


Figure 5. The aerosol surface forcing efficiencies (β) estimated by the direct method for the both TOD and SOD at 60° solar zenith angle from the combination of each instrument-measured AOD and SSI: (a) direct, (b) diffuse, (c) $\text{global}_{\text{shaded}}$, and (d) $\text{global}_{\text{unshaded}}$ irradiances. The TOD and SOD represent total observation data and simultaneous observation data. See color version of this figure at back of this issue.

column water vapor amounts because these parameters alter the incident solar fluxes in the pristine atmosphere. Surface solar flux changes are also a strong function of the SZA. We estimated the surface albedo for the Gosan site (ocean surface type) from a parameterization developed by Taylor *et al.* [1996] because the upward flux was not measured at Gosan site during the ACE-Asia IOP. The surface albedo was set to 0.06 at a 60° SZA. The column-integrated water vapor amount and the temperature and pressure profiles are taken from balloon sounding data at Gosan weather station.

[39] Figure 6 shows plots of the daily mean values of three radiometer-derived ΔF of $\text{global}_{\text{shaded}}$ and $\text{global}_{\text{unshaded}}$ irradiance with the daily mean τ_{500} measured by the CMDL Sun photometer. We note that the ΔF are analyzed for SOD of the radiometers by the hybrid method. For all cases, the same F° was applied. The measured average global irradiance for 9 days (case study) given in Figure 6 is 502.4, 492.7 and 492.4 Wm^{-2} for CMDL, SIO and METRI, respectively. The calculated mean ΔF is -53.7 , -62.7 and -62.9 Wm^{-2} for the same data sets. A 2.0% difference in the measured SSI translated into differences of 16.8–19.0% in ΔF . The deviations of ΔF in this study that result from differences in the global irradiance measurement methods are comparable to that of Sathesh and Ramanathan [2000]. The difference in the monthly mean ΔF between $\text{global}_{\text{shaded}}$ and $\text{global}_{\text{unshaded}}$ irradiance measurements is about 19.8%.

[40] The reason for this variance in ΔF and the associated β can be explained by the performance of each instrument under a broad range of aerosol loadings. The histogram in Figure 6 shows the frequency of occurrence (%) of τ_{500} at 0.1 intervals. In the majority range of AOD, 0.3–0.5 (about 72.3% of total data points), SIO and METRI have a very similar ΔF values which are 12.1 Wm^{-2} larger than the CMDL ΔF . During high aerosol-laden periods, $\tau_{500} > 0.6$, the magnitude of ΔF values for the three set of instruments followed in the following order: $\text{CMDL} < \text{SIO} < \text{METRI}$. On a very clean, low aerosol loading, day on 16 April, the METRI SSI was higher than the other two instruments,

resulting in a lower ΔF . The trend in the ΔF difference between CMDL and SIO is relatively constant over the range of AOD values. The CMDL ΔF is lower than that of SIO for all AOD ranges. The METRI ΔF is lower for $\text{AOD} < 0.1$ and is higher than others for $\text{AOD} > 0.6$. This trend in the METRI ΔF increased the slope for the regression of ΔF versus AOD. The slope of the linear regression lines, β , in Figure 6, is -154.2 , -150.8 , -177.2 for CMDL, SIO, METRI, respectively. CMDL β is about 4.5% higher than SIO. However, the METRI β is about 10% and 14% higher

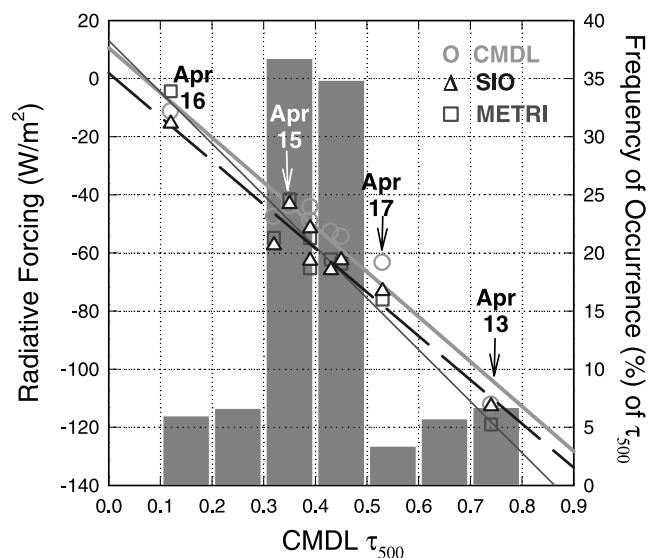


Figure 6. Daily mean values of three radiometer-derived ΔF , for coincident observation data of CMDL $\text{global}_{\text{shaded}}$ and SIO $\text{global}_{\text{unshaded}}$ and METRI $\text{global}_{\text{unshaded}}$ irradiances, is plotted with daily mean τ_{500} measured by the CMDL Sun photometer. The slope is β : CMDL (thick solid line), SIO (dashed line), and METRI (thin solid line). Histogram shows the frequency of occurrences (%) of AOD at 0.1 intervals of τ_{500} .

Table 5. Comparison of Aerosol Surface Forcing Efficiencies ($\text{Wm}^{-2}/\tau_{500}$) at 60° Solar Zenith Angle Between a Direct Method Using Measurement Data and a Hybrid Method Which Uses Both Model and Measurement Data^a

AOD	Direct		Diffuse		Global _{shaded} CMDL	Global _{unshaded}	
	CMDL	SIO	CMDL	SIO		SIO	METRI
	<i>Direct Method</i>						
CMDL	-418.33 (·)	-413.72 (-1.1)	128.36 (·)	127.65 (-4.8)	-80.22 (·)	-79.61 (-0.8)	-85.53 (6.6)
METRI	-402.43 (-3.8)	-400.69 (-4.2)	125.93 (-1.9)	122.38 (-0.6)	-75.73 (-5.6)	-78.41 (-0.8)	-84.50 (5.3)
AERONET	-420.02 (0.4)	-412.11 (-1.5)	128.63 (0.2)	128.15 (-4.7)	-82.56 (2.9)	-79.09 (-2.3)	-88.30 (10.1)
	<i>Hybrid Method</i>						
CMDL	-417.10 (-0.3)	-414.48 (-0.9)	128.16 (-0.2)	127.46 (-0.7)	-80.67 (0.6)	-80.07 (-1.4)	-85.97 (7.2)
METRI	-402.99 (-3.7)	-401.27 (-4.8)	125.78 (-2.0)	122.24 (-4.8)	-75.94 (-5.3)	-78.62 (-0.2)	-84.71 (5.6)
AERONET	-409.62 (-2.1)	-401.70 (-4.0)	129.28 (0.7)	128.76 (0.3)	-75.03 (-6.5)	-71.59 (10.8)	-80.80 (0.7)

^aThe percent deviation of aerosol surface forcing efficiency relative to the combination of CMDL AOD and CMDL SSI in parentheses. Periods within parentheses are the reference from which the percent deviations of the other values in parentheses are calculated.

than that of CMDL and SIO. These deviations of β are comparable to other ACE-Asia results of β at Gosan. β was calculated as $-73.0 \text{ Wm}^{-2}/\tau_{500}$ using the hybrid method [Bush and Valero, 2003], $-77.6 \text{ Wm}^{-2}/\tau_{500}$ by an NCAR CRM simulation [Won et al., 2004] and $-63.9 \text{ Wm}^{-2}/\tau_{500}$ averaged from four methods [Nakajima et al., 2003]. All methods calculated β for a 60° solar zenith angle. Bush and Valero [2003] and Won et al. [2004] differ by 4.6 Wm^{-2} based on τ at 500 nm. However, the difference between Won et al. [2004] and Nakajima et al. [2003] is $13.7 \text{ Wm}^{-2}/\tau_{500}$ (20% deviation). In these studies, differences in β can arise from different analytical methods, observation data and slightly different analysis periods. However, these deviations stress the necessity of more accurate and reliable measurements of aerosol optical properties and SSI to improve the confidence of radiation model simulation and satellite data analysis.

5.3. Comparison of Direct and Hybrid Method Results

[41] The β determined by the two methods, direct and hybrid approach described in 5.1 and 5.2, are comparable to one another. Table 5 shows β at 60° SZA for SOD estimated by the two methods. Little variance is observed in calculating the β between direct and hybrid methods except for the combination of the AERONET AOD and direct and global irradiances. The slight differences in β between the direct and hybrid methods may be due to variations in the column water vapor and atmospheric gas concentrations in the radiative transfer calculations for an aerosol-free atmosphere. However, a distinct discrepancy in β is observed between the measurement data for different instruments. The maximum deviation between instruments relative to the result from the combination of CMDL AOD and CMDL SSI is about 4.8%, 4.8%, 6.5% and 10.8% for direct, diffuse, global_{shaded} and global_{unshaded} irradiances, respectively.

6. Summary and Conclusions

[42] We compared aerosol optical depths (AOD) and surface shortwave irradiances (SSI) measured from three Sun photometers and sets of radiometers at Gosan during the ACE-Asia field campaign in April 2001. We also quantified the effects of the uncertainties in the AOD and SSI estimates of aerosol surface radiative forcing (ΔF) and forcing efficiency (β). The principal findings of our analysis are summarized below:

[43] 1. The 500 nm AOD (τ_{500}) ranged from 0.05 to 1.0 at Gosan over the course of the ACE-Asia campaign. The mean (τ_{500}) shows a good agreement within 0.014 (3.6%). However, bias and root mean square differences of this study over a broad range of aerosol loadings are larger than previous comparison studies.

[44] 2. In spite of good statistical agreements, the CMDL Sun photometer showed lower AOD values under high AOD (>0.7) conditions, but higher values in clean conditions (<0.2) than that of other instruments. Instantaneous differences of τ_{500} between instruments were as large as 0.09 on a heavy dust day and may be due to differences in daily cleaning and tracking errors as well as measurement elevation of the instruments.

[45] 3. Over the course of the comparison, the mean difference of SSI was 1.6, 11.7 and 10.1 Wm^{-2} for direct, diffuse and global irradiance, respectively. However, an 8% difference on a heavy dust day (DOY 103) between direct radiometers was apparent. Distinct diurnal variations in the absolute differences of diffuse and global irradiances were prevalent on most days and is likely due to a difference in the cosine angular response of the instruments.

[46] 4. The mean β s and associated deviations, which were estimated by the combinations of different instrument-derived AODs and SSIs, for simultaneous observation data at 60° solar zenith angle over a 24 hour time period are -411.14 ± 10.6 , 126.46 ± 5.68 , -79.50 ± 3.92 and $-82.57 \pm 5.70 \text{ Wm}^{-2}/\tau_{500}$ for direct, diffuse, global_{shaded} and global_{unshaded} irradiances, respectively.

[47] 5. The effect of AOD and SSI (in parenthesis) on β , which was estimated by the direct method, relative to the mean value is about 4.3% (1.8%), 4.8% (2.7%), 8.6% and 3.2% (10.7%) for direct, diffuse, global_{shaded} and global_{unshaded} irradiance, respectively.

[48] 6. A 2.0% difference in the measured global irradiance for a given 9 days in this study caused differences of 16.8–19.0% in ΔF . These differences in ΔF between instruments caused about 4.5%–14.0% deviations in β .

[49] 7. The maximum deviation of β at 60° solar zenith angle due to a combined errors of AOD and SSI measurements is about 4.8%, 4.8% 6.5% and 10.8% for direct, diffuse, global_{shaded} and global_{unshaded}, respectively.

[50] In this study, the discrepancies among instruments on several dusty days degraded the short-term comparisons of AOD and SSI, and ΔF and β derivations. However, this dependence on dust days might be reduced in long-term

analyses. Further long-term measurement with more careful calibration, field maintenance and analysis should help to quantify and reduce the observational uncertainties in climate aerosol forcing.

[51] **Acknowledgments.** This research was supported by the BK21 program and by the Climate Environment System Research Center sponsored by the SRC program. We thank the NOAA office global programs for support of the CMDL measurement. Comments from Robert Stone and J.-G. Won are also acknowledged.

References

- Bates, T. S., B. J. Huebert, J. L. Gras, F. B. Griffiths, and P. A. Durekee (1998), International Global Atmospheric Chemistry (IGAC) Project's First Aerosol Characterization Experiment (ACE 1): Overview, *J. Geophys. Res.*, *103*, 16,297–16,318.
- Bokoye, A. I., A. Royer, N. T. O'Neill, P. Cliche, G. Fedosejevs, P. M. Teillet, and L. J. B. McArthur (2001), Characterization of atmospheric aerosols across Canada from a ground-based Sun photometer network: AEROCAN, *Atmos. Ocean*, *39*, 429–456.
- Bush, B. C., and F. P. J. Valero (2002), Spectral aerosol radiative forcing at the surface during the Indian Ocean Experiment (INDOEX), *J. Geophys. Res.*, *107*(D19), 8003, doi:10.1029/2000JD000020.
- Bush, B. C., and F. P. J. Valero (2003), Aerosol Radiative Forcing at Gosan during the ACE-Asia campaign, *J. Geophys. Res.*, *108*(D23), 8660, doi:10.1029/2002JD003233.
- Charlson, R. J., S. E. Schwartz, J. M. Hales, R. D. Cess, J. A. Coakley Jr., J. E. Hansen, and D. J. Hoffmann (1992), Climate forcing by anthropogenic aerosols, *Science*, *255*, 423–430.
- Chou, M.-D., and W. Zhao (1997), Estimation and model validation of surface solar radiation and cloud radiative forcing using TOGA COARE measurements, *J. Clim.*, *10*, 610–620.
- De La Casinière, A., A. I. Bokoye, and T. Cabot (1997), Direct solar spectral irradiance measurements and updated simple transmittance models, *J. Appl. Meteorol.*, *36*, 509–520.
- Dubovik, O., and M. D. King (2000), A flexible inversion algorithm for retrieval of aerosol optical properties from Sun and sky radiance measurements, *J. Geophys. Res.*, *105*, 20,673–20,696.
- Dubovik, O., A. Smirnov, B. N. Holben, M. D. King, Y. J. Kaufman, T. F. Eck, and I. Slutsker (2000), Accuracy assessments of aerosol optical properties retrieved from Aerosol Robotic Network (AERONET) Sun and sky radiance measurements, *J. Geophys. Res.*, *105*, 9791–9806.
- Dutton, E. G., P. R. Steve, and J. J. DeLuise (1994), Features and effects of aerosol optical depth observed at Mauna Loa, Hawaii: 1982–1992, *J. Geophys. Res.*, *99*, 8295–8306.
- Dutton, E. G., J. J. Michalsky, T. Stoffel, B. W. Forgan, J. Hickey, D. W. Nelson, T. L. Alverta, and I. Reda (2001), Measurement of broadband diffuse solar irradiance using current commercial instrumentation with a correction for thermal offset errors, *J. Atmos. Oceanic Technol.*, *19*, 297–314.
- Halthore, R. N., S. Nemesure, S. E. Schwartz, D. G. Imre, A. Berk, E. G. Dutton, and M. H. Bergin (1998), Models overestimate diffuse clear-sky surface irradiance: A case for excess atmospheric absorption, *Geophys. Res. Lett.*, *25*, 3591–3594.
- Holben, B. N., et al. (1998), AERONET—A federal instrument network and data archive for aerosol characterization, *Remote Sens. Environ.*, *66*, 1–16.
- Huebert, B. J., T. Bates, P. B. Russell, G. Shi, Y. J. Kim, K. Kawamura, G. Carmichael, and T. Nakajima (2003), An overview of ACE-Asia: Strategies for quantifying the relationships between Asian aerosols and their climatic impacts, *J. Geophys. Res.*, *108*(D23), 8633, doi:10.1029/2003JD003550.
- Kato, S., T. P. Akerman, E. E. Clothiaux, J. H. Mather, G. G. Mace, M. L. Wesely, F. Murcray, and J. Michalsky (1997), Uncertainties in modeled and measured clear-sky surface shortwave irradiances, *J. Geophys. Res.*, *102*, 25,881–25,898.
- Kim, D.-H., B.-J. Sohn, T. Nakajima, T. Takemura, T. Takemura, B.-C. Choi, and S.-C. Yoon (2004), Aerosol optical properties over east Asia determined from ground-based sky radiation measurements, *J. Geophys. Res.*, *109*, D02209, doi:10.1029/2003JD003387.
- Markowicz, K. M., P. J. Flatau, P. K. Quinn, C. M. Carrico, M. K. Flatau, A. M. Vogelmann, and M. Liu (2003), Influence of relative humidity on aerosol radiative forcing, *J. Geophys. Res.*, *108*(D23), 8662, doi:10.1029/2002JD003066.
- McArthur, L. J. B., D. H. Halliwell, O. J. Niebergall, N. T. O'Neill, J. R. Slusser, and C. Wehrli (2003), Field comparison of network Sun photometers, *J. Geophys. Res.*, *108*(D19), 4596, doi:10.1029/2002JD002964.
- Michalsky, J., E. Dutton, M. Rubes, D. Nelson, T. Stoffel, M. Wesley, M. Splitt, and J. Dlusisi (1999), Optimal measurement of surface shortwave irradiance using current instrumentation, *J. Atmos. Oceanic Technol.*, *16*, 55–69.
- Michalsky, J. J., et al. (2003), Result from the first ARM diffuse horizontal shortwave irradiance comparison, *J. Geophys. Res.*, *108*(D3), 4108, doi:10.1029/2002JD002825.
- Min, H.-K., J. Kim, B.-C. Choi, and S.-N. Oh (2002), Characteristics of spectral aerosol optical depth retrieved from ground-based Sun photometer measurements in Seoul, Korea: An application of cloud screen algorithm (CSA) (in Korean), *J. Kor. Meteorol. Soc.*, *38*, 25–28.
- Mitchell, R. M., and B. W. Forgan (2003), Aerosol measurement in the Australian Outbreak: Intercomparison of Sun photometers, *J. Atmos. Oceanic Technol.*, *20*, 54–66.
- Nakajima, T., et al. (2003), Significance of direct and indirect radiative forcings of aerosols in the east China Sea region, *J. Geophys. Res.*, *108*(D23), 8658, doi:10.1029/2002JD003261.
- Ohmura, A., et al. (1998), Baseline Surface Radiation Network (BSRN)/WCRP, a new precision radiometry for climate research, *Bull. Am. Meteorol. Soc.*, *79*, 2115–2136.
- Philippa, R. (2002), Underestimation of solar global and diffuse radiation measured at Earth's surface, *J. Geophys. Res.*, *107*(D22), 4654, doi:10.1029/2002JD002396.
- Raes, F., T. Bates, F. M. McGovern, and M. V. Liedekerke (2000), The second Aerosol Characterization Experiment (ACE-2): General overview and main results, *Tellus, Ser. B*, *52*, 111–126.
- Ramanathan, V., et al. (2001), Indian Ocean Experiment: An integrated analysis of the climate forcing and effects of the great Indo-Asian haze, *J. Geophys. Res.*, *106*, 28,371–28,398.
- Ricchiazzi, P., S. Yang, C. Gautier, and D. Sowle (1998), SBDART: A research and teaching software tool for plane-parallel radiative transfer in the Earth's atmosphere, *Bull. Am. Meteorol. Soc.*, *79*, 2102–2114.
- Russell, P. B., J. M. Livingston, P. Hignett, S. Kinne, J. Wong, A. Chien, P. Durekee, and P. V. Hobbs (1999), Aerosol-induced radiative flux changes off the United States mid-Atlantic coast: Comparison of values calculated from Sun photometer and in situ data with those measured by airborne pyranometer, *J. Geophys. Res.*, *104*, 2289–2307.
- Satheesh, S. K., and V. Ramanathan (2000), Large difference in tropical aerosol forcing at the top of the atmosphere and Earth's surface, *Nature*, *405*, 60–63.
- Schmid, B., J. Michalsky, R. Halthore, M. Beauharnois, L. Harrison, J. Livingston, P. Russell, B. Holben, T. Eck, and A. Smirnov (1999), Comparison of aerosol optical depth from four solar radiometers during the fall 1997 ARM intensive observation period, *Geophys. Res. Lett.*, *26*(17), 2725–2728.
- Schwartz, S. E., and M. O. Andrea (1996), Uncertainty in climate change caused by aerosols, *Science*, *272*, 1121–1122.
- Smirnov, A., B. N. Holben, T. F. Eck, O. Dubovik, and I. Slutsker (2000), Cloud screening and quality control algorithm for the AERONET database, *Remote Sens. Environ.*, *73*, 337–349.
- Taylor, J. P., J. M. Edwards, M. D. Glew, P. Hignett, and A. Slingo (1996), Studies with a flexible new radiation SODE. II: Comparisons with aircraft short-wave observations, *Q. J. R. Meteorol. Soc.*, *122*, 839–861.
- Won, J.-G., S.-C. Yoon, S.-W. Kim, A. Jefferson, E. G. Dutton, and B. Holben (2004), Estimation of direct radiative forcing of Asian dust aerosols with Sun/sky radiometer and lidar measurements at Gosan, Korea, *J. Meteorol. Soc. Jpn.*, *82*, 115–130.
- Yoon, S.-C., J.-G. Won, and S.-W. Kim (2001), Ground-based micro-pulse lidar monitoring of aerosols at Gosan during ACE-Asia IOP, paper presented at First ACE-Asia Data Workshop, Calif. Inst. of Technol., Pasadena, Calif., 29 Nov. to 1 Dec.
- E. G. Dutton, A. Jefferson, and J. A. Ogren, NOAA Climate Monitoring and Diagnostics Laboratory, R/CMDL-1, 325 Broadway, Boulder, CO 80305, USA. (anne.jefferson@noaa.gov)
- B. N. Holben, NASA Goddard Space Flight Center, Mail code 923, Greenbelt, MD 20771, USA.
- J. Kim, S.-W. Kim, and S.-C. Yoon, School of Earth and Environmental Studies, Seoul National University, 56-520 San 56-1, Sillim-dong, Gwanak-gu, Seoul, Republic of Korea 151742.
- F. P. J. Valero, Scripps Institution of Oceanography, University of California, San Diego, 9500 Gilman Drive, La Jolla, CA 92093-0242, USA.

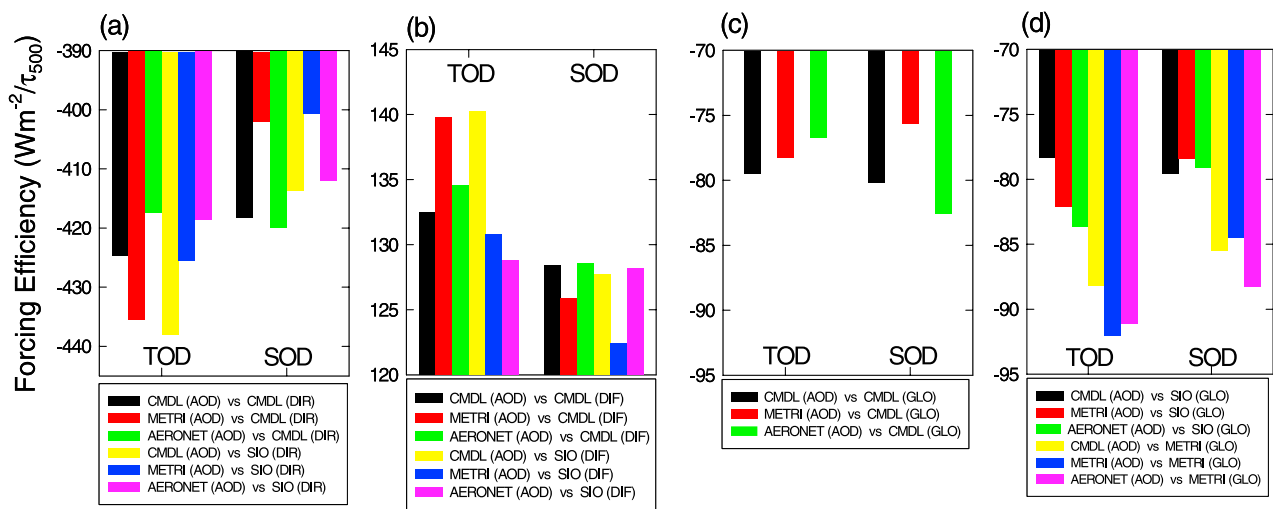


Figure 5. The aerosol surface forcing efficiencies (β) estimated by the direct method for the both TOD and SOD at 60° solar zenith angle from the combination of each instrument-measured AOD and SSI: (a) direct, (b) diffuse, (c) global_{shaded}, and (d) global_{unshaded} irradiances. The TOD and SOD represent total observation data and simultaneous observation data.